

Metabolic fate of peptides in a rice protein hydrolysate in rat intestine and blood after oral administration

Satoshi Miyauchi^a, Shiro Kajiwara^b and Kenji Sato^{a*}

^aDivision of Applied Biosciences, Graduate School of Agriculture, Kyoto University, Kitashirakawa Oiwake-cho, Kyoto 606 8502, Japan

^bBansyu chomiryo Co., Ltd., 948, Nozato, Himeji, Hyogo 670 0811, Japan

*Corresponding author: Kenji Sato, Division of Applied Biosciences, Graduate School of Agriculture, Kyoto University, Kitashirakawa Oiwake-cho, Kyoto 606 8502, Japan. Tel: +81-75-753-6444; E-mail: sato.kenji.7x@kyoto-u.ac.jp

DOI: 10.31665/JFB.2022.18327

Received: October 14, 2022; Revised received & accepted: December 16, 2022

Citation: Miyauchi, S., Kajiwara, S., and Sato, K. (2022). Metabolic fate of peptides in a rice protein hydrolysate in rat intestine and blood after oral administration. J. Food Bioact. 20: 40–55.

Abstract

The objective of this study was to elucidate the metabolic fate of peptides in a rice protein hydrolysate (RPH) in rats. Peptides present in RPH and its *in vitro* exopeptidase digest were identified using liquid chromatography-tandem mass spectrometry. One hour after an oral administration of RPH (250 mg/kg body weight), the levels of *in vitro* exopeptidase-resistant pyroglutamyl peptides in the lumen and ileal tissue significantly increased, whereas those of exopeptidase-susceptible peptides remained unchanged. Among them, the concentrations of pyroGlu-Leu, pyroGlu-Val, and pyroGlu-Lys significantly yet slightly increased in portal blood, while those of other hydrophilic ones (pyroGlu-Gln, pyroGlu-Glu, etc.) remained unchanged. However, all of the pyroglutamyl peptides were stable in rat ileal extract and blood plasma. These findings indicate that the pyroglutamyl peptides can enter enterocytes and resist to peptidases, while small amounts are transported to the blood, suggesting that pyroglutamyl peptides in enterocytes might be returned to the lumen.

Keywords: Rice protein hydrolysates; Pyroglutamyl peptides; Bioavailability; Peptide, LC-MS/MS.

1. Introduction

It has been demonstrated that food protein hydrolysates exert beneficial effects on human health beyond simply serving as amino acids sources (Yoshikawa et al., 2000; Chakrabarti et al., 2018). Peptides in food protein hydrolysates have been proposed to impart specific beneficial effects by acting as ligands for receptors, enzyme inhibitors, antioxidants, etc. Based on this concept, most bioactive peptides have been identified using *in vitro* activity-guided fractionation. For example, *in vitro* angiotensin I-converting enzyme (ACE) inhibitory activity has been widely used to identify potential anti-hypertensive peptides. Indeed, some ACE inhibitory peptides exert anti-hypertensive effects in animal models (Yang et al., 2003; Matsui et al., 2004; Aluko, 2015). Furthermore, some human clinical trials have demonstrated that oral administration of food protein hydrolysates exert anti-hypertensive effects (Kawasaki et al., 2000; Dong

et al., 2013). However, blood concentrations (1–5 nM) of the ACE inhibitory peptides (Shen and Matsui, 2017; Sato, 2022) were far lower than the concentration (1–100 μM) used for *in vitro* assays (Lee and Hur, 2017), which suggests that these peptides might exert anti-hypertensive effects via mechanisms other than ACE inhibition (Tanaka et al., 2006; Liao et al., 2018). Alternatively, unidentified peptides in food protein hydrolysates or their metabolites may be responsible for the anti-hypertensive effect. Therefore, food-derived active peptides in the target organs should be comprehensively characterized in order to understand the underlying mechanism. However, except for food-derived collagen and elastin peptides (Iwai et al., 2005; Shigemura et al., 2012), food-derived peptides in the body, such as blood and tissue extracts, are difficult to detect directly owing to their low concentrations. To overcome this problem, we have proposed a two-step approach for their identification. First, indigestible peptides were identified in the *in vitro* exopeptidase digest of food protein hydrolysates, which is much easier than the direct

identification of peptides in biological material owing to the abundance of peptides and lower interference of the matrix in the in vitro digest. Second, the identified indigestible peptides were detected in the target organ after oral administration of food protein hydrolysates using a liquid chromatography-tandem mass spectrometry (LC-MS/MS) in multiple reaction monitoring (MRM) mode. Using this approach, food-derived peptides were identified in human blood after the ingestion of corn and wheat gluten hydrolysates (Ejima et al., 2018). In this study, di- and tripeptides consisting of proline and/or pyroglutamic acid were resistant to the in vitro exopeptidase digestion. Pyroglutamyl peptides are generated non-enzymatically from peptides with glutamyl residue at the amino terminus during the preparation of food protein hydrolysates (Sato et al., 1998). Short-chain pyroglutamyl peptides are resistant to endo- and exopeptidases digestion (Sato et al., 1998; Ejima et al., 2018). For the in vitro exopeptidase digestion, Ejima et al. used carboxypeptidase A, a major exopeptidase in pancreatic juice, and leucine aminopeptidase, which is widely distributed as an intracellular enzyme in organs such as the liver, kidney, intestine (Sanderink et al., 1988). However, the levels of some indigestible peptides in the in vitro exopeptidase digest did not increase in human blood after ingestion of corn and wheat gluten hydrolysates (Ejima et al., 2018). Furthermore, little is known regarding the metabolic fate of the food-derived peptides in the digestive tract. The objective of the present study was to elucidate the metabolic fate of food-derived peptides in the small intestine and blood of rats after oral administration of rice protein hydrolysate (RPH).

2. Materials and methods

2.1. Rice protein hydrolysate

A rice protein hydrolysate (RPH) was obtained from Bansyu Chomiryo (Hyogo, Japan). Briefly, rice protein was suspended in water and digested with food-grade microbial and plant proteases. The reaction was terminated by boiling. The liquid phase was collected, concentrated under vacuum, and spray dried.

2.2. Reagents

Acetonitrile (HPLC grade) and phosphate buffered saline (pH 7.4, 10× PBS) was purchased from Nacalai Tesque (Kyoto, Japan). Porcine leucine aminopeptidase, bovine carboxypeptidase A, and N_ε-acetyl-L-lysine were purchased from Sigma-Aldrich (St. Louis, MO, USA). N,N-dimethylformamide, 4-methylmorpholine, piperidine, *t*-butyl methyl ether, trifluoroacetic acid, amino acids mixture standard solution (type H), and phenyl isothiocyanate were purchased from Fujifilm Wako Pure Chemical (Osaka, Japan). Benzotriazol-1-yl-oxytrypyrrolidinophosphonium hexafluorophosphate (PyBop), 1-hydroxybenzotriazole (Hobt), 9-fluorenylmethoxycarbonyl (Fmoc) amino acid derivatives, L-pyroglutamic acid, Fmoc amino acid-bonded *p*-alkoxybenzyl alcohol (Alko) resin, and proline-bound 2-chlorotriptyl resin were purchased from Watanabe Chemical (Hiroshima, Japan). 6-aminoquinolyl-*N*-hydroxysuccinimidyl carbamate (AccQ) was purchased from Toronto Research Chemicals (Toronto, ON, Canada).

2.3. In vitro exopeptidase digestion of peptides in rice protein hydrolysate (RPH)

Exopeptidase digestion of RPH was performed as previously de-

scribed (Chen et al., 2019), with slight modifications. RPH was dissolved in PBS at a final concentration of 2.5 mg/mL. Leucine aminopeptidase (2.45 U) and carboxypeptidase A (7.7 U) were added to the RPH solution (1 mL). Digestion was performed at 37 °C for 4 h. After 4 h, enzymes were removed by ultrafiltration using an Amicon Ultra 10 K device (Merck, Darmstadt, Germany). The effluent was collected and used as the in vitro exopeptidase digest.

2.4. Identification of peptides in RPH and in vitro exopeptidase digest

Peptides in RPH and its exopeptidase digest were fractionated by size exclusion chromatography (SEC) using a Superdex Peptide 10/300 GL column (GE Healthcare, Chicago, IL, USA). The column was equilibrated with 0.1% formic acid containing 10% acetonitrile at a flow rate 0.5 mL/min. Aliquots (200 μL) of the RPH solution (2.5 mg/mL) and exopeptidase digest were loaded into the column. Fractions were collected every 1 min. Aliquots (100 μL) of each fraction were dried under vacuum and the amino and imino groups of the peptides in each fraction were derivatized with AccQ. The residue was dissolved in 20 μL of 20 mM HCl, and added to 60 μL of 50 mM sodium borate buffer (pH 8.8) and 20 μL of 0.3% AccQ acetonitrile solution, and then incubated at 50 °C for 10 min. The product was mixed with 50 μL of 5 mM sodium phosphate buffer (pH 7.5) containing 5% acetonitrile and clarified by filtration with a Cosmonice filter (4 mm i.d., 0.45 μm, Nacalai Tesque). Aliquots of the filtrate (10 μL) were injected to a liquid chromatography-electrospray ionization tandem mass spectrometer (LC-MS/MS, LCMS 8040, Shimadzu, Kyoto, Japan). AccQ-peptides were resolved by reversed-phase high performance liquid chromatography (RP-HPLC) using an Inertsil ODS-3 column (2.1 mm i.d. × 250 mm, GL Science, Tokyo, Japan). A binary linear gradient was performed using 0.1% formic acid (solvent A) and 0.1% formic acid containing 80% acetonitrile (solvent B) at a flow rate of 0.2 mL/min. The gradient program was as follows; 0–3 min, 0% B; 3–20 min, 0–30% B; 20–30 min, 30–100% B; 30–35 min, 100% B; 35–35.1 min, 100–0% B; 35.1–45 min, 0% B. The column was maintained at 40 °C. AccQ-derivatives were specifically detected in the precursor ion scan mode by selecting the precursor ion that generated the AccQ-derived product ion (b1); mass to charge ratio (*m/z*) of 171.1, in positive mode by applying a collision energy of –35 eV to scan ranges of *m/z* = 250–300, 300–350, 350–400, 400–450, 450–500, and 500–600. The observed precursor ions of the AccQ-derivatives were further analyzed in the product ion scan mode at collision energies of –15 eV and –35 eV to estimate the peptide sequence.

To prepare the pyroglutamyl peptides fraction from the RPH solution and its exopeptidase digest, solid phase extraction using a strong cation exchanger (AG50W × 8, hydrogen form, 100–200 mesh, Bio-Rad Laboratories, Hercules, CA, USA) was carried out as described previously (Ejima et al., 2018). The non-absorbed effluent was collected as a pyroglutamyl peptides fraction. The pyroglutamyl peptides fraction (200 μL) was subjected to the SEC under the same condition as described above. Aliquots (10 μL) of the SEC fraction were subjected to the LC-MS under the same elution conditions without derivatization with AccQ. The pyroglutamyl peptides were detected in the precursor ion scan mode by selecting the precursor ion that generated the immonium ion of pyroglutamic acid (*m/z* = 84.1) in positive mode at a collision energy of –35 eV for scan ranges of *m/z* = 100–200, 200–250, 250–300, 300–350, 350–400, and 400–500 (for RPH), or 180–240, 240–300, 300–400, and 400–500 (for the exopeptidase digest). The observed precursor ions of the pyroglutamyl peptides were further analyzed using the product ion scan mode at collision energies of –15 eV

and -35 eV to estimate the peptide sequence.

To confirm the degradation of peptides larger than tripeptides in RPH after the *in vitro* exopeptidase digestion, the RPH solution and its exopeptidase digest were directly analyzed using LC-MS without AccQ derivatization under the same elution condition. The non-derivatized peptides and amino acids were detected by scanning the following scan ranges in total ion scan mode: $m/z = 50$ – 150 , 150 – 200 , 200 – 250 , 250 – 300 , 300 – 350 , 350 – 400 , 400 – 450 , 450 – 500 , 500 – 600 , 600 – 700 , 700 – 800 , and 800 – $1,000$.

2.5. Peptide synthesis

The estimated peptides were synthesized by adopting the Fmoc strategy using a peptide synthesizer (PSSM-8, Shimadzu). Isomers of Asp-X peptides (X: any amino acid residue) with L- and D-aspartyl residues, and α and β peptide bonds in each sequence, were synthesized using the method of Ejima et al. (2019). The synthetic peptides were purified by reversed-phase high performance liquid chromatography (RP-HPLC) using a Cosmosil 5C18MS-II column (10 mm i.d. \times 250 mm, Nacalai Tesque). A binary linear gradient was performed using 0.1% formic acid (solvent A) and 0.1% formic acid containing 80% acetonitrile (solvent B) at a flow rate of 2 mL/min. The gradient program was as follows: 0–20 min, 0–50% B; 20–30 min, 50–100% B; 30–35 min, 100% B; 35–35.1 min, 100–0% B; 35.1–45 min, 0% B. The column was maintained at 40 °C. Peptide elution was monitored by measuring the absorbance at 214 and 254 nm, and peptide purity was evaluated using LC-MS. The peptide concentration was determined by amino acids analysis following HCl hydrolysis. Amino acids were derivatized with phenyl isothiocyanate using the methods described by Bidlingmeyer et al. (1984) with slight modifications (Aito-Inoue et al., 2006).

2.6. Animal experiments

All animals used in this study were treated in accordance with the National Institutes of Health (NIH) guidelines for animal experiments. All experimental procedures were approved by the animal care committee of the Louis Pasteur Center for Medical Research (approval number 20201). Seven-week-old male Wistar/ST rats (210–230 g body weight) were purchased from Japan SLC (Shizuoka, Japan) and acclimatized to environmental conditions for 1 week. They were fed rodent chow (solid type of certified diet MF, Oriental Yeast, Tokyo, Japan), kept in a room at 24–26 °C and 40–60% humidity under a 12 h light-dark cycle, and could freely access diet and water. Rats were fasted for 16 h and divided into two groups: the control group ($n = 3$) and RPH group ($n = 3$). RPH was dissolved in PBS and administered using a sonde at 250 mg/kg body weight (BW). Blood was collected from the portal vein under isoflurane anesthesia 60 min after the administration of RPH (RPH group) and without RPH administration (control group). Plasma was prepared by centrifugation at 800 $\times g$ for 10 min in the presence of heparin. The small intestines were collected. The inner contents of the small intestine were flushed with 10 mL of PBS. The washed small intestines and their inner content were stored at -80 °C until further analysis.

2.7. Quantification of peptides in RPH and its exopeptidase digest

The RPH solution and its exopeptidase digest were diluted to 0.5

mg/mL with distilled water. Aliquots of these diluents (10 μ L) were derivatized with AccQ, as described above. The concentrations of the AccQ-derivatives and pyroglutamyl peptides were determined using LC-MS/MS in MRM mode under identical elution condition. The MRM conditions were optimized for synthetic peptides using the LabSolutions LCMS Ver. 5.5 (Shimadzu) using the synthetic peptides. The synthetic peptides were also used as external standards.

AccQ-derivatives of Asp-Phe, Asp-Ile/Leu, Asp-Glu, and Asp-Val isomers were resolved by RP-HPLC using the Inertsil ODS-3 column and detected in MRM mode. A shallower binary gradient was performed using 0.1% formic acid (solvent A) and 0.1% formic acid containing 80% acetonitrile (solvent B) at a flow rate of 0.2 mL/min. The gradient program was as follows: 0–20 min, 5% B; 20.1–45 min, 10% B; 45.1–80 min, 13% B; 80–82 min, 13–100% B; 82–90 min, 100% B; and 90.1–100 min, 5% B.

2.8. Quantification of RPH-derived peptides in the lumen, ileal tissue, and portal vein blood of rats

The effluent from the small intestine was centrifuged at 800 $\times g$ for 10 min to obtain the supernatant. The supernatant was mixed with three volumes of ethanol and centrifuged at 12,000 $\times g$ for 10 min. The deproteinized supernatant was collected and used as the ethanol-soluble fraction of lumen. The ileum was thoroughly rinsed with PBS and cut into small pieces. The pieces (100 mg) were homogenized in PBS (100 μ L) using a BioMasher II (Nippi, Tokyo, Japan). The homogenate was mixed with three volumes of ethanol and centrifuged at 12,000 $\times g$ for 10 min. The ethanol-soluble fraction was then collected. Plasma was mixed with three volumes of ethanol, and the ethanol-soluble fraction was obtained under the same conditions as described above.

Aliquots of the ethanol-soluble fractions (50 μ L) were dried under vacuum and derivatized with AccQ, as described above. The AccQ-derivatives and pyroglutamyl peptides were quantified using LC-MS/MS in MRM mode under the same conditions.

2.9. Digestion of peptides by proteases in rat plasma and ileal extract

Rat plasma and the small intestine were prepared from eight-week-old male Wistar/ST rat. The ileum with mucosa was dissected, and its inner contents was thoroughly washed with PBS. The pieces were homogenized in nine volumes of PBS. The homogenates were centrifuged at 12,000 $\times g$ for 10 min at 4 °C, and the supernatants were used as the crude proteases for the digestion of peptides.

Synthetic peptides (pyroGlu-Gln, pyroGlu-Glu, pyroGlu-Ala, pyroGlu-Leu, pyroGlu-Lys, and Ser-Gln) were mixed with rat plasma or ileum extracts at a concentration of 50 μ M and incubated at 37 °C. Aliquots (20 μ L) were withdrawn after 0, 1, 3, and 6 h of incubation and mixed with three volumes ethanol. After centrifuging the mixture at 12,000 $\times g$ for 10 min at 4 °C, the supernatant was collected. The remaining peptides in the ethanol-soluble fraction were quantified using LC-MS/MS.

2.10. Statistical analysis

Statistical analyses were performed using a R (version 3.5.1). The difference between the means of the two groups was evaluated using Student's *t*-test, and a *p*-value of less than 0.05 was considered statistically significant.

3. Results

3.1. Identification of peptides in RPH and its exopeptidase digest

Peptides in RPH and its exopeptidase digest were first fractionated using SEC, followed by RP-HPLC. MS/MS in precursor ion scan mode was used for detection. Elution patterns of RPH and its exopeptidase digest in SEC mode (Figure S1) and all mass chromatograms for the AccQ-derivatives and pyroglutamyl peptides in RPH and its digest are shown in Figures S2–5. In SEC mode, some peaks were eluted after elution of water (41 min). Thus, fractions were collected by 70 min. Tryptophan was eluted at 70 min. LC-MS/MS analyses revealed that peptides were eluted to 48 min (Tables 1–4). Figure 1 shows a mass chromatogram of the AccQ-derivatives of SEC fraction (Fr.) 37 of RPH in the scanning range of m/z 350–400 and the spectra of product ions arising from precursor ion with $m/z = 389$, 359, and 373, in peak 15, 18, and 19, respectively. These precursor ions were analyzed in a product ion scan mode with collision energies of -35 eV and -15 eV. These product ions were assigned to the a, b, c and x, y, z ions from the peptide according to definition by Papayannopoulos (1995). Immonium ions of amino acid residues were detected and are indicated with a one-letter abbreviation of amino acid along with an asterisk. AccQ-derived b1 ion ($m/z = 171$) was observed for all the AccQ-derivatives. Based on the precursor and products ions, compounds composed of precursor ions of $m/z = 389$ (peak 15), $m/z = 359$ (peak 18), and $m/z = 373$ (peak 19) were assigned as AccQ-Ser-Leu/Ile, AccQ-Gly-Leu/Ile, and AccQ-Ala-Leu/Ile, respectively. The assigned peptide sequence based on the precursor and product ions of the AccQ-derivatives of RPH and its exopeptidase digest are summarized in Tables 1 and 2, respectively. Before in vitro exopeptidase digestion, forty-four di- and tripeptides with branched-chain amino acids were observed (Table 1). After the exopeptidase digestion, these peptides disappeared, and the prolyl and aspartyl dipeptides remained. (Table 2). Peptides larger than tripeptides were detected in the non-AccQ-derivatives of RPH using LC-MS, while it was difficult to detect these larger peptides in the AccQ-derivatives using LC-MS/MS analysis in precursor ion scan mode. After the exopeptidase digestion, most of the larger peptides disappeared (Figure S6).

Figure 2 shows a mass chromatogram of pyroglutamyl peptide in SEC Fr.37 of RPH with a scanning range at m/z 200–250 and spectrum of product ions arising from a precursor ion with $m/z = 243$ in peak 4. This precursor ion was analyzed by product ion scan mode. Immonium ion derived from pyroglutamic acid (pE*, $m/z = 84$) was also observed. Based on precursor and product ions, the compound composed of precursor ion $m/z = 243$ was assigned as pyroGlu-Leu/Ile. The assigned sequences of the pyroglutamyl peptides and related compounds in RPH and its exopeptidase digest are summarized in Tables 3 and 4, respectively. Before exopeptidase digestion, tetrapeptides were observed; after exopeptidase digestion, only di- and tripeptides were detected (Figure S6).

The assigned peptides in RPH with high peak areas (>3 million counts for AccQ-derivatives and >1 million counts for pyroglutamyl peptides) in single ion monitoring (SIM) mode were synthesized and used to confirm the estimated sequence and quantification. By contrast, all assigned peptides in the exopeptidase digest were synthesized, except for the pyroglutamyl peptides, which showed extremely low peak areas. To estimate sequence of peptides consisting of Ile or Leu, all possible peptides were synthesized, and successfully resolved using RP-HPLC (data not shown). Thus, Ile or Leu containing peptides were identified by comparison with the retention times of the analogous synthetic peptides. All peptides showed the same retention times and precursor and

product ion patterns as those synthesized ones using LC-MS/MS in MRM mode, confirming the accuracy of the estimated sequence.

Figure 3 shows the peptide concentrations in RPH and its exopeptidase digest. It is apparent that Ser-Gln, Ala-Gln, Ala-Leu, Ala-Ala, Ser-Glu, Ser-Leu, and Asp-Phe were the major dipeptides constituting RPH (≈ 10 – 20 $\mu\text{mol/g}$). Most of the peptides were completely degraded by the in vitro exopeptidase digestion for 4 h; however, dipeptides with pyroglutamyl residue or aspartic residue at the amino terminus, such as pyroGlu-Gln, pyroGlu-Glu, pyroGlu-Leu, and Asp-Val, remained after the exopeptidase digestion (>5 $\mu\text{mol/g}$). The levels of pyroGlu-Gln and pyroGlu-Leu increased after exopeptidase digestion, indicating that these peptides were generated from longer peptides such as pyroGlu-Gln-Leu and pyroGlu-Leu-Leu during the exopeptidase digestion. These exopeptidase-resistant peptides were detected in other exopeptidase digests of plant protein hydrolysates (Ejima et al., 2018; Chen et al., 2019).

As shown in Figure 4, dipeptides with an aspartic residue at the amino terminus gave some minor peaks using the shallow gradient elution of LC-MS/MS in MRM mode. The main peaks were identical to the retention times of normal L- α -Asp-X peptides. Some minor peaks corresponding to L- β -Asp-X and D- β -Asp-X were also observed. In addition, some proline-containing peptides (Gly-Pro, Glu-Pro, etc.) remained after exopeptidase digestion.

3.2. Presence of RPH-derived peptides inside the small intestine, ileal tissue, and blood plasma of rats after oral administration of RPH

Figure 5 shows the concentrations of the peptides containing amino groups in the lumen, ileal tissue, and plasma of rat. Unexpectedly, even before RPH administration, most of the peptides were detected inside the small intestine (Figure 5a), which were possibly derived from endogenous and microbial proteins. Some peptides were also detected in ileal tissue and portal blood plasma before the administration (Figure 5b, c). Nevertheless, the concentrations of these peptides did not significantly increase inside the intestine after oral administration of RPH, which is consistent with the observation that most peptides with amino groups were degraded by in vitro exopeptidase digestion (Figure 5d). The concentrations of Gly-Leu and Ala-Ser in the ileal tissue (Figure 5b) and Gly-Leu and Asn-Leu in the plasma from portal vein blood (Figure 5c) significantly yet slightly increased after administration.

Figure 6 shows the pyroglutamyl peptide concentrations in rats before and after oral administration of RPH. In contrast with no increase of the peptides containing amino groups (Figure 5a), the concentrations of most of the pyroglutamyl peptides significantly increased inside the small intestine (Figure 6a), owing to their resistance to the in vitro exopeptidase digestion. Exopeptidase-susceptible pyroglutamyl peptides such as pyroGlu-Gln-Leu-Leu were not detected in the lumen. The composition of pyroglutamyl peptides in the ileal tissue (Figure 6b) was similar to that in the lumen (Figure 6a). One hour after administration of RPH, pyroGlu-Leu, pyroGlu-Lys, and pyroGlu-Val levels significantly increased to ≈ 10 – 70 nM in the plasma from portal vein blood (Figure 6c). However, even after the administration of RPH, pyroGlu-Gln and pyroGlu-Glu were not detected in the portal vein blood plasma, while these peptides were abundant in the lumen and ileal tissue after administration of RPH (Figure 6d).

3.3. Digestion of peptides by crude proteases in rat blood and small intestine

The susceptibility of several synthetic peptides (pyroGlu-Leu, py-

Table 1. Summary of estimated peptide sequences of AccQ-derivatives in RPH

Peak No.	SEC Fr.	Estimated peptide sequence	Precursor ions (<i>m/z</i>)	Product ions (<i>m/z</i>)
1	36	AS	347	170.9 (AccQ, b1), 176.9 (y1), 213.9 (a2), 242.0 (b2)
2	36	SA	347	60.5 (Ser*), 171.0 (AccQ, b1), 177.2 (y2), 257.8 (b2)
3	36, 37	AA	331	161.0 (y2), 171.0 (AccQ, b1), 241.8 (b2)
4	36	GQ	374	84.1 (Gln**), 146.7 (y1), 170.9 (AccQ, b1), 203.7 (y2), 227.8 (b2)
5	36	AN	374	44.4 (Ala*), 132.9 (y1), 170.9 (AccQ, b1), 203.9 (y2), 214.1 (a2), 241.7 (b2)
6	36	AQ	388	44.5 (Ala*), 147.0 (y1), 170.9 (AccQ, b1), 213.9 (y2), 217.9 (y2), 241.9 (b2)
7	36	AT	361	44.0 (Ala*), 119.7 (y1), 171.0 (AccQ, b1), 190.8 (y2), 213.7 (a2), 242.1 (b2)
8	36	AE	389	148.1 (y1), 170.9 (AccQ, b1), 213.9 (a2), 219.0 (y2), 242.1 (b2)
9	36	TA	361	170.9 (AccQ, b1), 190.7 (y2), 272.1 (b2)
10	36	PA	357	70.1 (Pro*), 171.0 (AccQ, b1), 186.9 (y2), 240.0 (a2)
11	36	VS	375	72.3 (Val*), 171.0 (AccQ, b1), 205.0 (y2), 242.0 (a2), 270.2 (b2)
12	36	VT	389	72.2 (Val*), 170.9 (AccQ, b1), 218.8 (y2), 241.9 (a2), 269.8 (b2)
13	36	VA	359	72.2 (Val*), 170.9 (AccQ, b1), 189.0 (y2), 242.0 (a2), 269.9 (b2)
14	36	IS, LS ¹	389	86.1 (Ile/Leu*), 171.0 (AccQ, b1), 219.0 (y2), 256.0 (a2), 283.6 (b2)
15	36, 37	SI, SL ¹	389	171.0 (AccQ, b1), 219.0 (y2), 258.0 (b2)
16	36	IA, LA ¹	373	86.1 (Ile/Leu*), 170.9 (AccQ, b1), 203.0 (y2), 255.9 (a2), 283.9 (b2)
17	36	VV	387	72.4 (Val*), 170.8 (AccQ, b1), 217.0 (y2), 242.1 (a2), 270.3 (b2)
18	37	GI, GL ¹	359	170.9 (AccQ, b1), 188.9 (y2), 227.9 (b2)
19	37	AI, AL ¹	373	132.1 (y1), 170.9 (AccQ, b1), 203.1 (y2), 213.9 (a2), 241.9 (b2)
20	42–45	GF	393	171.0 (AccQ, b1), 227.9 (b2)
21	36, 37	SQ	404	60.2 (Ser*), 83.6 (Gln**), 147.0 (y1), 170.9 (AccQ, b1), 233.8 (y2), 230.0 (a2), 257.8 (b2)
22	36	DT ²	405	74.2 (Thr*), 171.1 (AccQ, b1), 234.7 (y2), 258.2 (a2)
23	36	EQ ²	446	83.8 (Glu**, Gln**), 147.2 (y1), 171.1 (AccQ, b1), 272.3 (a2), 275.5 (y2), 299.6 (b2)
24	36, 37	TE	419	74.4 (Thr*), 84.4 (Glu**), 147.7 (y1), 170.8 (AccQ, b1), 243.7 (a2), 248.7 (y2)
25	36	GVS	432	72.1 (Val*), 106.1 (y1), 170.9 (AccQ, b1), 199.9 (a2), 228.1 (b2), 327.1 (b3), 385.6 (a4)
26	36	GVA	416	72.4 (Val*), 90.1 (y1), 170.9 (AccQ, b1), 188.8 (y2), 200.0 (a2), 228.1 (b2), 327.0 (b3)
27	36	VQ	416	71.9 (Val*), 101.1 (Gln*), 147.1 (y1), 171.0 (AccQ, b1), 242.1 (a2), 245.8 (y2), 269.8 (b2)
28	36	GIS, GLS ²	446	86.3 (Ile/Leu*), 106.1 (y1), 171.0 (AccQ, b1), 199.7 (a2), 228.0 (b2), 276.0 (y3), 340.6 (b3)
29	36, 37	VE	417	72.0 (Val*), 148.2 (y1), 170.9 (AccQ, b1), 242.1 (a1), 246.9 (y2), 270.1 (b2)
30	36	GAI, GAL ²	430	44.3 (Ala*), 86.3 (Ile/Leu*), 132.1 (y1), 171.2 (AccQ, b1), 228.1 (b2), 259.8 (y2)
31	36	IQ, LQ ¹	430	84.1 (Gln**), 86.2 (Ile/Leu*), 146.9 (y1), 170.8 (AccQ, b1), 256.1 (a2), 259.8 (y2), 283.9 (b2)
32	36	IT, LT ²	403	86.2 (Ile/Leu*), 119.7 (y1), 171.0 (AccQ, b1), 232.5 (y2), 255.9 (a2)
33	36, 37	TI, TL ¹	403	86.1 (Ile/Leu*), 170.9 (AccQ, b1), 233.0 (y2), 272.0 (b2)
34	36, 37	IV, LV ¹	401	86.0 (Ile/Leu*), 171.1 (AccQ, b1), 230.9 (y2), 255.8 (a2), 284.0 (b2)
35	36, 37	VI, VL ¹	401	72.1 (Val*), 170.8 (AccQ, b1), 231.1 (y2), 242.3 (a2), 269.8 (b2)
36	36, 37	MI, ML ¹	433	86.2 (Ile/Leu*), 104.2 (Met*), 171.0 (AccQ, b1), 274.0 (a2)
37	36, 37	II, IL, LI, LL ¹	415	86.2 (Ile/Leu*), 171.0 (AccQ, b1), 244.9 (y2), 284.1 (b2)
38	37	NE ²	432	87.7 (Asn*), 101.7 (Glu*), 171.0 (AccQ, b1), 256.9 (a2), 261.9 (y2), 285.0 (b2)
39	37	SE	405	60.4 (Ser*), 147.8 (y1), 171.0 (AccQ, b1), 234.9 (y2)
40	37	SM ²	407	150.0 (y1), 170.9 (AccQ, b1), 236.9 (y2), 257.7 (b2)
41	37	NI, NL ¹	416	87.0 (Asn*), 132.0 (y1), 171.0 (AccQ, b1), 245.9 (y2), 256.8 (a2), 284.9 (b2)
42	37	DI, DL ¹	417	86.3 (Ile/Leu*), 131.7 (y1), 170.9 (AccQ, b1), 247.1 (y2), 286.0 (b2)
43	37	EI, EL ¹	431	84.1 (Glu**), 86.2 (Ile/Leu*), 132.4 (y1), 170.8 (AccQ, b1), 261.0 (y2), 271.9 (a2), 299.8 (b2)

Table 1. Summary of estimated peptide sequences of AccQ-derivatives in RPH - (continued)

Peak No.	SEC Fr.	Estimated peptide sequence	Precursor ions (m/z)	Product ions (m/z)
44	37	IM, LM ²	433	86.3 (Ile/Leu*), 170.8 (AccQ, b1), 256.1 (a2), 263.1 (y2), 284.3 (b2)
45	41–43	SF	423	119.9 (Phe*), 166.0 (y1), 171.0 (AccQ, b1), 230.0 (a2), 253.0 (y2), 258.0 (b2)
46	41, 42	TF	437	74.2 (Thr*), 166.0 (y1), 170.9 (AccQ, b1), 243.7 (a2), 267.0 (y2), 271.9 (b2)
47	41–43	AF	407	120.1 (Phe*), 165.9 (y1), 171.0 (AccQ, b1), 213.8 (a2), 236.9 (y2), 241.9 (b2)
48	41–43	VF	435	72.1(Val*), 170.9 (AccQ, b1), 242.0 (a2), 264.9 (y2), 270.0 (b2)
49	42–45	IF, LF ¹	449	86.2 (Ile/Leu*), 119.5 (Phe*), 171.0 (AccQ, b1), 256.1 (a2), 279.1 (y2), 283.8 (b2)
50	43	SY	439	60.4 (Ser*), 136.1 (Tyr*), 171.0 (AccQ, b1), 182.1 (y1), 229.7 (a2), 257.9 (b2), 269.1 (y2)
51	43	AY	423	171.0 (AccQ, b1), 182.0 (y1), 213.8 (a2), 241.9 (b2)
52	36	STS	464	59.7 (Ser*), 106.1 (y1), 171.2 (AccQ, b1), 219.9 (a2), 257.6 (b2)
53	36, 37	GVE ²	474	148.0 (y1), 170.8 (AccQ, b1), 227.9 (b2), 303.6 (y3)
54	36, 37	GIN, GLN ²	473	85.8 (Ile/Leu*), 87.3 (Asn*), 133.1 (y1), 171.1 (AccQ, b1), 199.5 (a2), 227.8 (b2), 303.1 (y3)
55	36	GIT, GLT ²	460	85.9 (Ile/Leu*), 119.8 (y1), 170.9 (AccQ, b1), 199.6 (a2), 228.1 (b2), 290.1 (y3), 340.6 (b3)
56	36	ASI, ASL ¹	460	44.1 (Ala*), 59.6 (Ser*), 85.7 (Ile/Leu*), 171.0 (AccQ, b1), 241.4 (b2), 289.5 (y3), 329.2 (b3)
57	36	AVI, AVL ¹	472	44.4 (Ala*), 71.9 (Val*), 170.4 (AccQ, b1), 214.1 (a2), 241.7 (b2), 301.7 (y3), 340.9 (b3)
58	36	IAI, IAL, LAI, LAL ²	486	86.2 (Ile/Leu*), 170.7 (AccQ, b1), 283.7 (b2), 315.9 (y3), 355.3 (b3)
59	37–41	SGF	480	60.6 (Ser*), 120.5 (Phe*), 165.9 (y1), 170.4 (AccQ, b1), 222.8 (y2), 258.2 (b2)
60	37, 38	GTF ²	494	73.9 (Thr*), 119.7 (Phe*), 165.8 (y1), 227.7 (b2), 267.1 (y2), 300.7 (a3), 323.7 (y3)
61	37–40	GAF ²	464	120.0 (Phe*), 166.0 (y1), 170.8 (AccQ, b1), 227.9 (b2)
62	37–42	FQ ²	464	84.5 (Gln**), 119.9 (Phe*), 147.4 (y1), 170.7 (AccQ, b1), 289.6 (a2), 318.2 (b2)
63	37	AAF ²	478	166.0 (y1), 170.8 (AccQ, b1), 241.8 (b2), 307.7 (y3)
64	37	GII, GIL, GLI, GLL ²	472	86.0 (Ile/Leu*), 131.9 (y1), 170.7 (AccQ, b1), 200.2 (a2), 227.9 (b2), 340.8 (b3)
65	41	GGF ²	450	120.1 (Phe*), 165.9 (y1), 171.1 (AccQ, b1), 199.7 (a2), 227.8 (b2), 279.8 (y3), 285.0 (b3)
66	41	DF	451	88.2 (Asp*), 171.0 (AccQ, b1), 257.7 (a2), 280.7 (y2), 285.9 (b2)
67	41	FE ²	465	119.9 (Phe*), 147.9 (y1), 171.0 (AccQ, b1), 294.6 (y2), 317.6 (b2)
68	41, 42	GVF ²	492	72.0 (Val*), 119.4 (Phe*), 166.0 (y1), 171.0 (AccQ, b1), 199.8 (a2), 227.9 (b2), 326.5 (b3)
69	42	YQ ²	480	83.8 (Gln**), 100.7 (Gln*), 136.0 (Tyr*), 147.0 (y1), 170.8 (AccQ, b1), 305.9 (a2), 333.6 (b2)
70	42–44	NF ²	450	86.6 (Asn*), 165.8 (y1), 170.8 (AccQ, b1), 284.9 (b2)
71	42–44	EF ²	465	84.0 (Glu**), 102.1 (Glu*), 120.2 (Phe*), 165.9 (y1), 171.0 (AccQ, b1), 299.8 (b2)
72	43–45	TY	453	74.0 (Thr*), 136.0 (Tyr*), 271.8 (b2), 282.7 (y2)
73	44, 45	VY ²	451	72.3 (Val*), 170.9 (AccQ, b1), 241.9 (a2), 269.8 (b2), 280.6 (y2)
74	36	STE ²	506	59.9 (Ser*), 74.1 (Thr*), 147.6 (y1), 170.9 (AccQ, b1), 229.5 (a2), 257.7 (b2), 335.6 (y3)
75	36	LTE, ITE ²	532	85.8 (Ile/Leu*), 147.7 (y1), 170.9 (AccQ, b1), 255.5 (a2), 361.6 (y3), 385.2 (b3)
76	36	TPI, TPL ¹	500	69.7 (Pro*), 85.7 (Ile/Leu*), 132.2 (y1), 170.5 (AccQ, b1), 228.8 (y2), 271.8 (b2), 330.1 (y3)
77	36	IIQ, ILQ, LIQ, LLQ ¹	543	86.1 (Ile/Leu*), 100.8 (Gln*), 147.1 (y1), 171.0 (AccQ, b1), 256.0 (a2), 284.0 (b2), 372.9 (y3), 396.9 (b3)
78	37	DVI, DVL ¹	516	85.9 (Ile/Leu*), 171.0 (AccQ, b1), 285.6 (b2), 384.9 (b3)
79	37, 38	IAF, LAF ¹	520	86.0 (Ile/Leu*), 165.6 (y1), 171.0 (AccQ, b1), 236.4 (y2), 256.1 (a2), 283.8 (b2), 354.7 (b3)
80	41–44	NIF, NLF ¹	563	86.1 (Ile/Leu*), 119.7 (Phe*), 170.8 (AccQ, b1), 257.1 (a2), 284.9 (b2), 397.8 (b3)
81	41–44	SIF, SLF ¹	536	60.2 (Ser*), 86.1 (Ile/Leu*), 119.9 (Phe*), 165.6 (y1), 170.9 (AccQ, b1), 229.7 (a2), 371.0 (b3)

¹Presence of both peptides consisting of Leu and Ile were confirmed by comparison with synthetic peptides. ²The identities of the tentatively assigned peptides were not confirmed, as their ion intensity was low in single ion monitoring mode. Supplemental Figure 1 shows the mass chromatograms with peak numbers.

Table 2. Summary of estimated peptide sequences and amino acid derivatives of AccQ-derivatives in the exopeptidase digest of RPH

Peak No.	SEC Fr.	Estimated peptide sequence	Precursor ions (<i>m/z</i>)	Product ions (<i>m/z</i>)
1	36	GP	343	69.7 (Pro*), 116.2 (y1), 171.1 (AccQ, b1), 228.0 (b2)
2	36	GV	345	171.0 (AccQ, b1), 175.0 (y2), 228.0 (b2)
3	34, 35	N-acetyllysine	359	84.0, 127.8, 171.0, 189.1
4	35	SP	373	115.9 (y1), 171.0 (AccQ, b1), 202.6 (y2), 230.2 (a2), 258.2 (b2)
5	35	AP	357	70.0 (Pro*), 116.0 (y1), 171.0 (AccQ, b1), 187.1 (y2)
6	35	PS	373	70.0 (Pro*), 171.0 (AccQ, b1), 202.9 (y2), 240.0 (a2)
7	35	PP	383	70.0 (Pro*), 115.9 (y1), 171.0 (AccQ, b1), 212.9 (y2), 267.7 (b2)
8	35	PV	385	70.0 (Pro*), 171.0 (AccQ, b1), 215.1 (y2), 240.2 (a2), 268.1 (b2)
9	35	VV	387	72.0 (Val*), 118.3 (y1), 171.0 (AccQ, b1), 216.9 (y2), 241.9 (a2), 270.1 (b2)
10	35, 36	IP, LP ¹	399	86.0 (Ile/Leu*), 171.0 (AccQ, b1), 229.0 (y2), 256.2 (a2), 284.0 (b2)
11	36, 37	GQ	374	56.0 (Gln**), 84.3 (Gln**), 147.3 (y1), 171.0 (AccQ, b1), 200.4 (a2), 228.0 (b2)
12	34, 35	PQ	414	70.0 (Pro*), 171.0 (AccQ, b1), 243.8 (y2)
13	34	pEK	428	84.0 (pyroGlu*), 171.0 (AccQ, b1), 258.2
14	35	QP	414	84.1 (Gln*), 170.9 (AccQ, b1), 244.4 (y2), 299.1 (b2)
15	35, 36	DP	401	115.9 (y1), 171.0 (AccQ, b1), 231.0 (y2), 286.3 (b2)
16	35, 36	EP	415	83.6 (Glu**), 115.9 (y1), 171.0 (AccQ, b1), 271.8 (a2), 299.9 (b2)
17	35–37	DV	403	118.1 (y1), 171.0 (AccQ, b1), 233.2 (y2), 286.2 (b2)
18	35, 36	IV, LV ¹	401	86.1 (Ile/Leu*), 170.9 (AccQ, b1), 230.8 (y2), 255.9 (a2)
19	36	DE	433	88.0 (Asp*), 147.7 (y1), 170.9 (AccQ, b1), 262.8 (y2), 285.7 (b2)
20	36, 37	NP	400	115.9 (y1), 171.0 (AccQ, b1), 230.0 (y2), 256.7 (a2), 284.7 (b2)
21	36	DI, DL ¹	417	86.1 (Ile/Leu*), 170.9 (AccQ, b1), 247.1 (y2), 286.0 (b2)
22	37–42	FP	433	70.0 (Pro*), 116.2 (y1), 119.9 (Phe*), 170.9 (AccQ, b1), 290.3 (a2), 318.3 (b2)
23	39–48	YP	449	70.1 (Pro*), 115.8 (y1), 136.0 (Tyr*), 171.0 (AccQ, b1), 279.2 (y2), 306.2 (a2), 334.0 (b2)
24	39–42	DF	451	120.3 (Phe*), 166.2 (y1), 171.1 (AccQ, b1), 285.9 (b2)
25	44–48	TY	453	74.0 (Thr*), 170.9 (AccQ, b1), 272.3 (b2), 282.9 (y2)

¹Presence of both peptides consisting of Leu and Ile were confirmed by comparison with synthetic peptides. Supplemental Figure 2 shows the mass chromatograms with peak numbers.

Table 3. Summary of estimated sequence of pyroglutamyl peptides in RPH

Peak No.	SEC Fr.	Estimated peptide sequence	Precursor ions (<i>m/z</i>)	Product ions (<i>m/z</i>)
1	35, 36	pEA	201	44.3 (Ala*), 84.1 (pyroGlu*), 89.9 (y1), 154.8 (a2), 183.1 (b2)
2	36	pES ²	217	60.2 (Ser*), 84.3 (pyroGlu*), 106.0 (y1), 170.8 (a2), 198.9 (b2)
3	36	pEV	229	72.1 (Val*), 84.0 (pyroGlu*), 118.0 (y1), 183.0 (a2)
4	36–38	pEI, pEL ¹	243	84.2 (pyroGlu*), 86.3 (Ile/Leu*), 132.4 (y1), 197.2 (a2)
5	35–37	pEQ	258	84.1 (pyroGlu*), 147.1 (y1), 212.3 (a2), 240.0 (b2)
6	35	pEE	259	84.1 (pyroGlu*), 101.8 (Glu*), 148.1 (y1), 241.2 (b2)
7	41, 42	pEF	277	84.0 (pyroGlu*), 120.1 (Phe*), 165.9 (y1), 231.1 (a2), 259.3 (b2)
8	44, 45	pEY	293	84.1 (pyroGlu*), 136.1 (Tyr*), 182.1 (y1), 247.1 (a2)
9	33, 34	pEAQ ²	329	44.4 (A*), 84.1 (pyroGlu*), 100.8 (Q*), 147.0 (y1), 155.2 (a2), 183.3 (b2)
10	33	pEVA ²	300	44.4 (Ala*), 72.1 (Val*), 84.3 (pyroGlu*), 90.2 (y1), 183.0 (a2), 211.0 (b2)

Table 3. Summary of estimated sequence of pyroglutamyl peptides in RPH - (continued)

Peak No.	SEC Fr.	Estimated peptide sequence	Precursor ions (<i>m/z</i>)	Product ions (<i>m/z</i>)
11	33	pELS, pEIS ¹	330	60.2 (Ser*), 84.2 (pyroGlu*), 86.2 (Ile/Leu*), 106.0 (y1), 197.0 (a2), 225.1 (b2), 312.2 (b3)
12	35	pEAE ²	330	44.1 (Ala*), 83.8 (pyroGlu*), 102.3 (Glu*), 147.9 (y1), 154.9 (a2), 182.9 (b2), 219.0 (y2)
13	33, 34	pEQQ ²	386	84.1 (pyroGlu*), 101.2 (Gln*), 147.1 (y1), 257.6 (c2)
14	33, 34	pETQ ²	359	84.3 (pyroGlu*), 147.0 (y1), 185.2 (a2), 212.9 (b2), 230.1(c2)
15	33, 34	pEEQ ²	387	84.3 (pyroGlu*), 101.0 (Gln*), 102.3 (Glu*), 147.1 (y1), 212.8 (a2), 241.0 (b2),
16	33, 34	pEQE ²	387	84.3 (pyroGlu*), 102.3 (Glu*), 148.2 (y1), 211.8 (a2), 240.2 (b2)
17	33, 34	pETE ²	360	74.3 (Thr*), 84.0 (pyroGlu*), 102.2 (Glu*), 148.1(y1), 184.7 (a2), 212.8 (b2)
18	33, 34	pEVQ	359	72.4 (Val*), 84.3 (pyroGlu*), 147.2 (y1), 182.9 (a2), 211.3 (b2), 246.0 (y2)
19	33, 34	pEIQ, pELQ ²	371	84.3 (pyroGlu*), 86.3 (Ile/Leu*), 101.0 (Gln*), 147.1 (y1), 197.1 (a2), 225.2 (b2), 260.1(y2)
20	35	pEQI, pEQL ¹	371	84.0 (pyroGlu*), 86.1 (Ile/Leu*), 132.1 (y1), 212.0 (a2), 240.1 (b2), 324.9 (a3)
21	35–37	pEII, pEIL, pELI, pELL ¹	356	84.1 (pyroGlu*), 86.2 (Ile/Leu*), 132.2 (y1), 197.1 (a2), 225.1 (b2)
22	41	pEVY ²	392	72.3 (Val*), 84.2 (pyroGlu*), 136.0 (Tyr*), 182.1 (y1), 211.3 (b2),
23	32–33	pELSE, pEISE ¹	459	60.2 (S*), 84.0 (pyroGlu*), 86.0 (I/L*), 101.9 (E*), 148.0 (y1), 197.1 (a2), 225.0 (b2), 235.0 (y2), 283.9 (a3), 312.0 (b3)
24	32–34	pEQII, pEQIL, pEQLI, pEQLL ¹	484	83.9 (pyroGlu*), 86.1 (Ile/Leu*), 101.1 (Q*), 240.1 (b2), 245.0 (y2), 353.1 (b3)
25	37, 38	pEFQ	405	84.0 (pyroGlu*), 101.1 (Gln*), 120.1 (Phe*), 147.0 (y1), 231.1 (a2)
26	37, 38	pEQF ²	405	84.0 (pyroGlu*), 119.9 (Phe*), 166.0 (y1), 240.1 (b2)

¹Presence of both peptides consisting of Leu and Ile were confirmed by comparison with synthetic peptides. ²The identities of the tentatively assigned peptides were not confirmed, as their ion intensity was low in single ion monitoring mode. Supplemental Figure 3 shows the mass chromatograms with peak numbers.

roGlu-Lys, pyroGlu-Glu, pyroGlu-Gln, pyroGlu-Ala, and Ser-Gln) to proteases in the blood and ileal extracts of rat was examined. In both cases, Ser-Gln, one of the major dipeptides in RPH that was degraded during *in vitro* exopeptidase digestion and whose con-

centration did not significantly increase inside the small intestine, decreased to ≈10% after incubation with both plasma and ileal extract for 1 h (Figure 7a, b). By contrast, more than 80% of the pyroglutamyl dipeptides in the ileal extracts remained 6 h after (Figure

Table 4. Summary of estimated sequence of pyroglutamyl peptides and related compound in the exopeptidase digest of RPH

Peak No.	SEC Fr.	Estimated peptide sequence	Precursor ions (<i>m/z</i>)	Product ions (<i>m/z</i>)
1	36	pES ²	217	56.2 (pyroGlu**), 60.2 (Ser*), 84.1(pyroGlu*), 106.0 (y1), 199.3 (b2)
2	36, 37	pEV	229	72.0 (Val*), 84.0 (pyroGlu*), 118.0 (y1), 183.0 (a2)
3		two pyroGlu	259	
4	35–37	pEQ	258	56.1 (pyroGlu**, Gln**), 84.0 (pyroGlu*, Gln**), 146.8 (y1)
5	36, 37	pEE	259	55.9 (pyroGlu**), 84.0 (pyroGlu*), 102.0 (Glu*), 148.0 (y2), 241.0 (b2)
6	37, 38	pEI, pEL ¹	243	56.0 (pyroGlu**), 84.0 (pyroGlu*), 86.0 (Ile/Leu*), 128.9 (c1), 132.0 (y1), 197.0 (a2)
7	42–46	pEY	293	84.0 (pyroGlu*), 136.0 (Tyr*), 182.0 (y1), 247.0 (a2)
8	41–46	pEF	277	56.0 (pyroGlu**), 84.0 (pyroGlu*), 120.0 (Phe*), 166.0 (y1), 231.0 (a2)
9	34	pEQP	355	70.2 (Pro*), 84.0 (pyroGlu*), 100.8 (Gln*), 115.8 (y1), 239.9 (b2), 338.4 (b3)
10	34	pENS ²	331	60.0 (Ser*), 84.0 (pyroGlu*), 106.0 (y1), 198.0 (a2), 313.0 (b3)
11	35	pEDV ²	344	72.1 (Val*), 83.9 (pyroGlu*), 118.0 (y1), 227.0 (b2), 233.0 (y2), 298.3 (a3)

¹Presence of both peptides consisting of Leu and Ile were confirmed by comparison with synthetic peptides. ²The identities of the tentatively assigned peptides were not confirmed, as their ion intensity was low in single ion monitoring mode. Supplemental Figure 4 shows the mass chromatograms with peak numbers.

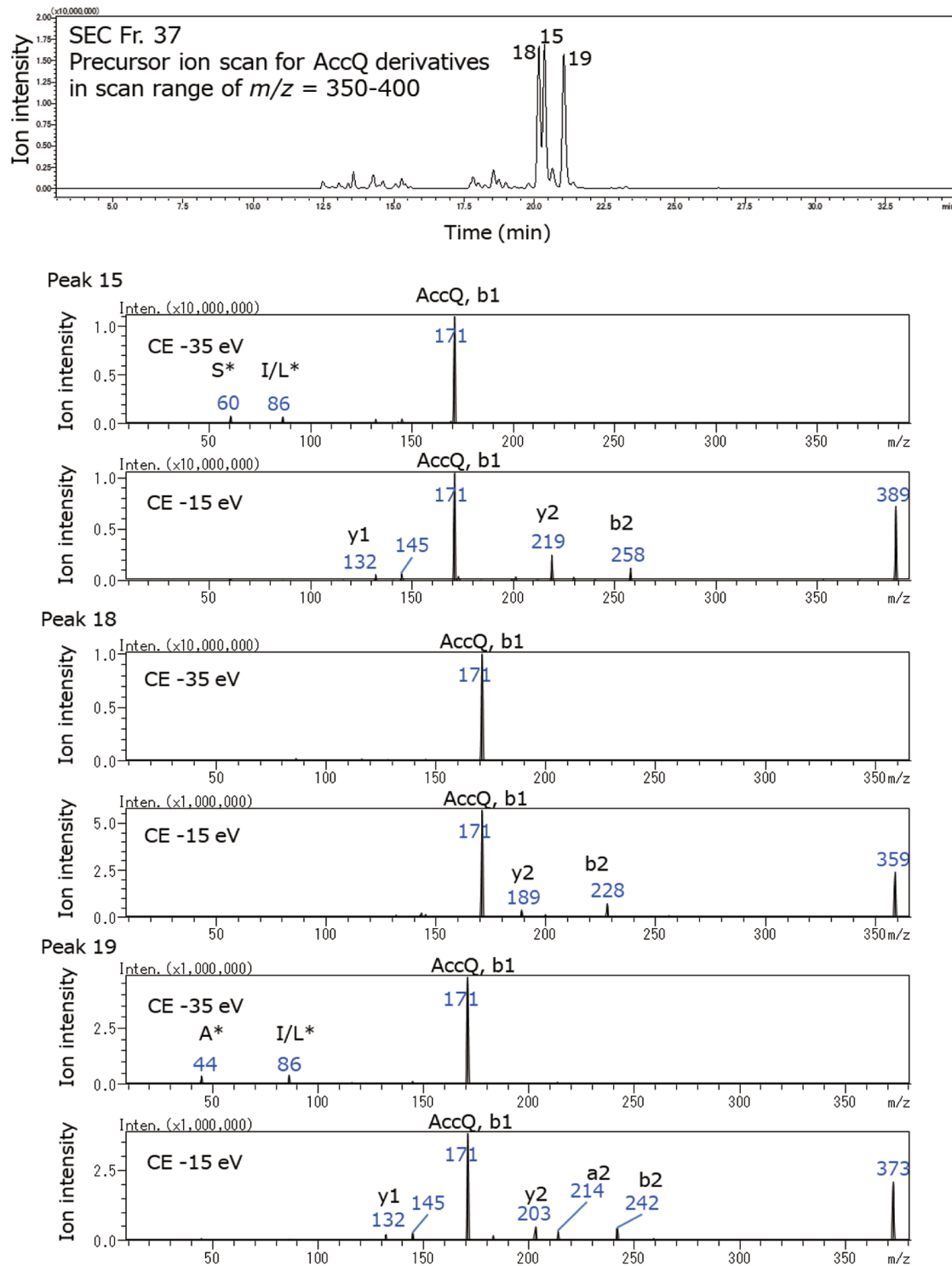


Figure 1. Mass chromatogram of AccQ-derivatives of SEC Fr. 37 of RPH in precursor ion scan mode (upper panel) and spectra of the product ions from precursor ions in peaks 18, 15, and 19, respectively (lower panels). The product ion scan was carried out using collision energies (CEs) at -35 and -15 eV. The immonium ions of amino acids are indicated as one-letter abbreviations with asterisk.

7a). PyroGlu-Gln, pyroGlu-Glu, and pyroGlu-Leu were also stable in the rat plasma for 6 h (Figure 7b). However, the pyroGlu-Ala and pyroGlu-Lys levels decreased to $\approx 50\%$ after incubation with

rat plasma for 3 h. These results indicate that peptides that resist carboxypeptidase A and leucine aminopeptidase, also resist to proteases in the ileum and the blood.

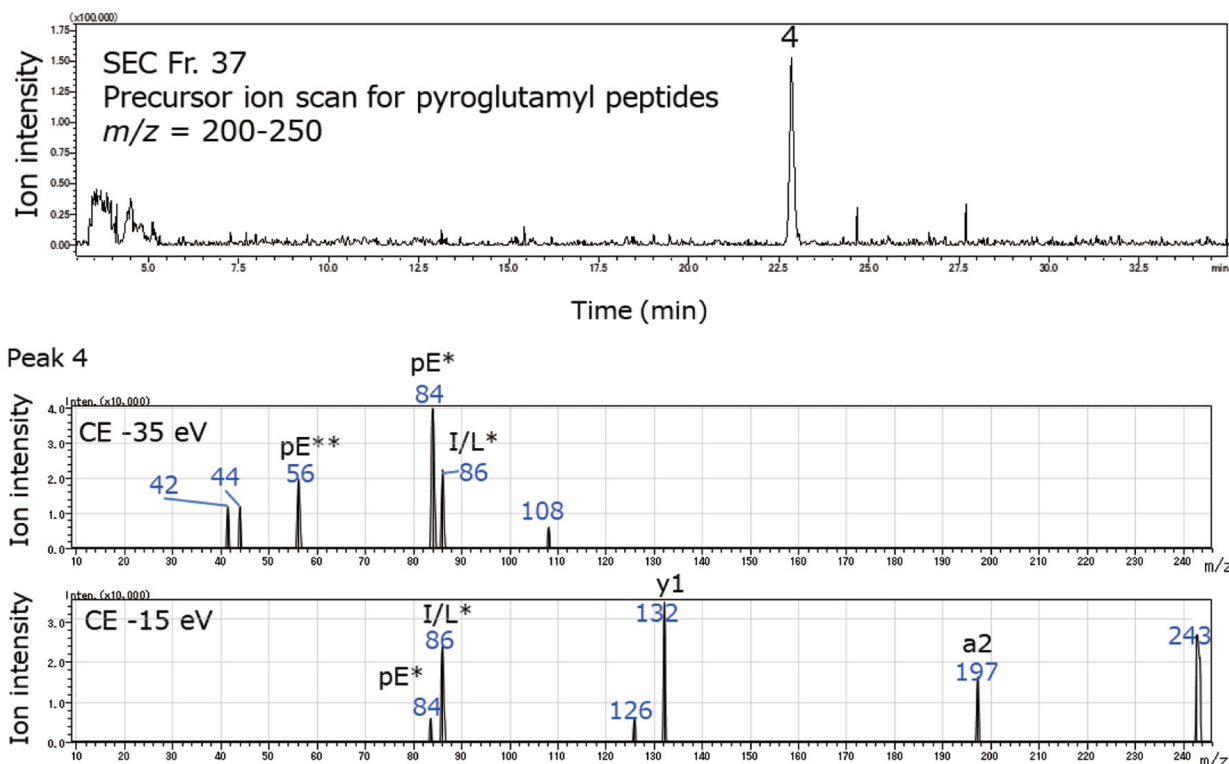


Figure 2. Mass chromatogram of a pyroglutamyl peptide of SEC Fr. 37 of RPH in precursor ion scan mode (upper panel) and spectra of product ions from the precursor ion in peak 4 (lower panels). The product ion scan was carried out using collision energies (CEs) at -35 and -15 eV. The immonium ions of amino acids are indicated as one letter abbreviation with asterisk. Pyroglutamyl residue is represented as pE. Immonium ions and related ions derived from pyroglutamic acid are indicated as pE with one and two asterisks, respectively.

4. Discussion

Sixty-three peptides with amino/imino groups and fourteen pyroglutamyl peptides were identified and quantified in RPH. Peptides larger than tripeptides were also detected in the RPH, most of which disappeared after *in vitro* exopeptidase digestion. Furthermore, most the amino group-containing short-chain peptides in RPH were degraded after *in vitro* exopeptidase digestion, except for peptides with a prolyl residue at the carboxy terminus or aspartyl residue at the amino terminus, which is consistent with the previously reported results (Ejima et al., 2018; 2019). Dipeptides containing aspartyl residue at amino terminus in an exopeptidase digest of porcine liver protein hydrolysate have been shown to exist four isomers with L- and D-aspartyl residues, and α and β peptide bonds in each sequence (Ejima et al., 2019). Although L/D- β -isomers were also found in Asp-Phe, Asp-Leu, Asp-Glu, and Asp-Val in RPH and its exopeptidase digest (Figure 4), their concentrations were less than those of L- α -Asp-X form; these finding are in contrast to those of a previous study (Ejima et al., 2019). The reason for this discrepancy remains to be elucidated. It is possible that the generation of the isomer of the aspartic dipeptides is dependent on the primary structure of the substrate protein and/or digestion conditions.

Even before the administration of RPH, some peptides containing amino groups were detected in the lumen. Sixty minutes after administration of RPH in a dose of 250 mg/kg BW, the peptide concentrations in the rats did not significantly increase, except for those of Gly-Leu, Ala-Ser, and Asn-Leu. These peptides were degraded by *in vitro* leucine aminopeptidase and carboxypeptidase

A digestion (Figure 3). In addition, Ser-Gln, a major short-chain peptide in RPH, was degraded by proteases in ileal tissue extract and blood plasma. Therefore, these peptides are continuously generated by the degradation of endogenous and microbial proteins and eliminated through exopeptidase digestion. Thus, RPH supplementation had only a small impact on the concentrations of the amino group-containing peptides in the body 1 h after the administration, while these peptides were detected in the body without administration.

Most of the pyroglutamyl peptides in RPH resisted *in vitro* exopeptidase digestion, with exception of pyroglutamyl tri- and tetrapeptides such as pyroGlu-Gln-Leu-Leu. After administration of RPH, the concentrations of most of the exopeptidase-resistant pyroglutamyl peptides significantly increased in the lumen and ileal tissue. The composition of pyroglutamyl peptides in the lumen was nearly identical to that in the ileal tissue after administration, which indicates that the pyroglutamyl dipeptides resist not only *in vitro* exopeptidase digestion but also *in vivo* exopeptidase digestion in the digestive tract. However, the composition of pyroglutamyl peptides in portal blood after administration was completely different from that in ileal tissue. Only the concentrations of pyroGlu-Leu, pyroGlu-Lys, and pyroGlu-Val significantly yet slightly (<70 nM) increased in the portal blood after administration of RPH, while those of pyroGlu-Gln and pyroGlu-Glu remained the same. Thus, we first speculated that pyroGlu-Gln and pyroGlu-Glu, which resist exopeptidase digestion in lumen, might be degraded by other exopeptidases in the enterocytes, extracellular matrix, and blood. However, pyroGlu-Gln and pyroGlu-Glu were stable in rat ileal extract and blood plasma for 6 h. These results

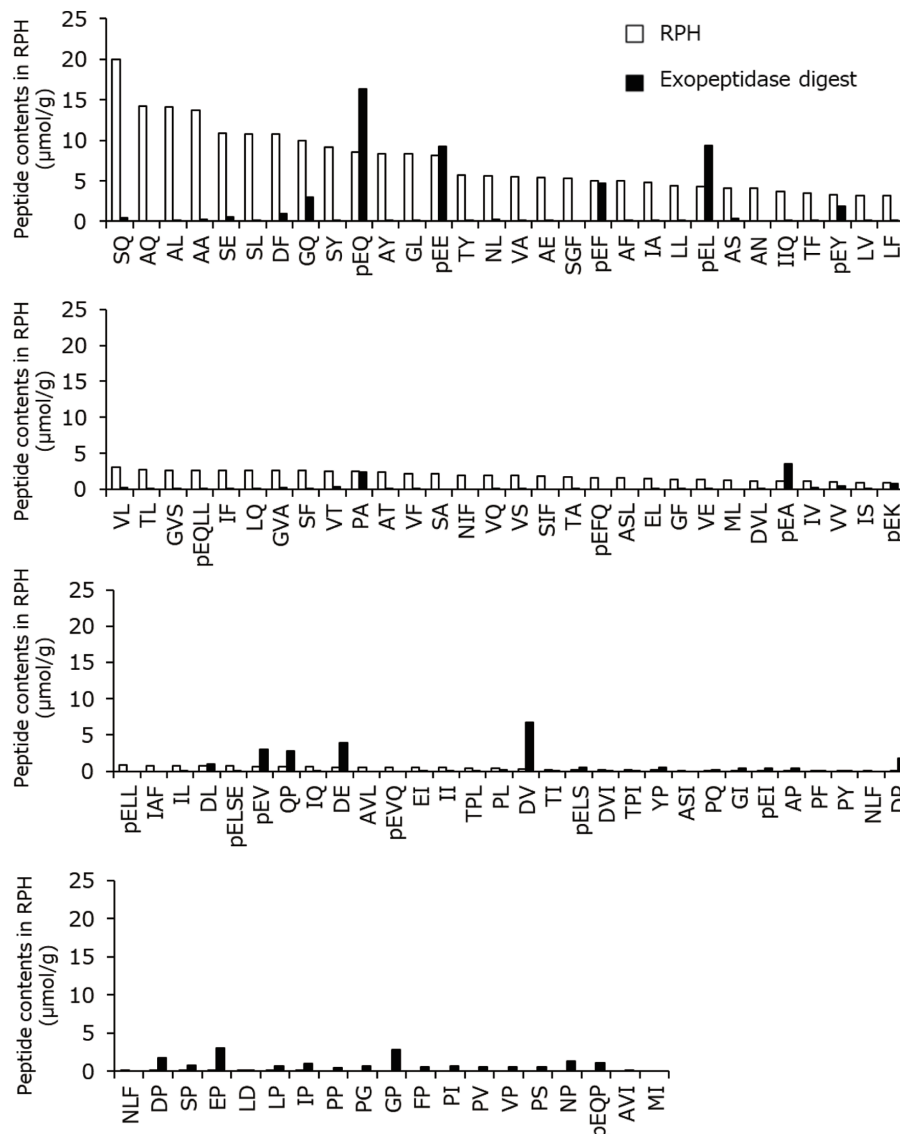


Figure 3. Concentrations of peptides in RPH and its exopeptidase digest. The amino acid residues are indicated as one letter abbreviations, and pE represents pyroglutamyl residue.

indicate that exopeptidases are not responsible for the disappearance of these pyroglutamyl peptides in the blood, and that these pyroglutamyl peptides in enterocytes are not transported into the bloodstream.

It has been demonstrated that the concentrations of certain peptides, such as prolylhydroxyproline (Pro-Hyp) and prolylglycine (Pro-Gly), significantly increase (>10 μM) in human blood after ingestion of collagen hydrolysate and elastin hydrolysate, respectively (Iwai et al., 2005; Shigemura et al., 2012). Thus, these peptides can pass through the enterocytes and enter the bloodstream. Di- and tripeptides are believed to be transported via peptide transporter 1 (Pept1) on the apical membrane of enterocytes (Shen and Matsui, 2017). Indeed, Pro-Hyp was shown to be transported via Pept1 on the porcine brush-border membrane (Aito-Inoue et al., 2007). Thus, peptides in enterocytes are assumed to be transported into the blood via transporters on the basolateral membrane. However, these basolateral peptide transporters have not yet been

clearly identified. By contrast, pyroGlu-His was shown to be transported via non-Pept1 transporter on the renal brush-border membrane (Skopicki et al., 1998). Therefore, pyroglutamyl peptides in the lumen can be transported into enterocytes via similar transporters on the renal brush-border membrane rather than Pept1. It has been demonstrated that the concentration of a hydrophobic pyroglutamyl peptide, pyroGlu-Leu, significantly increased in blood after administration (Sato et al., 2013), which is consistent with the result of the present study. However, after RPH administration, hydrophilic pyroglutamyl peptides, pyroGlu-Gln and pyroGlu-Glu, were not detected in the portal vein blood, although the concentration of them in the ileal tissue significantly increased. Thus, unidentified basolateral transporters may specifically recognize hydrophobic pyroglutamyl peptides such as pyroGlu-Leu and pyroGlu-Val. In addition, the concentrations of the hydrophilic pyroglutamyl peptide, pyroGlu-Lys, increased in the blood after RPH administration, although its concentration in RPH and its exopepti-

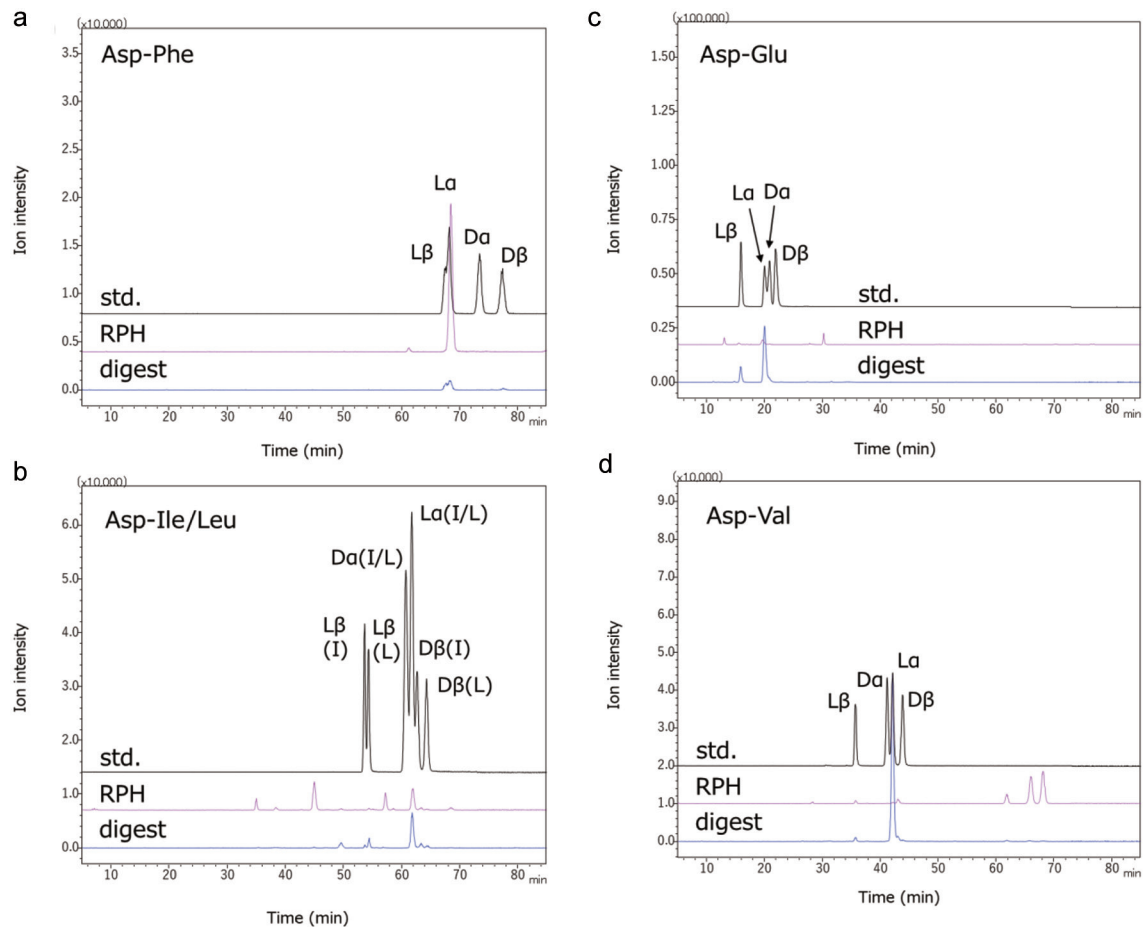


Figure 4. Isomers of di-peptides with aspartyl residue at the amino terminus in RPH and its exopeptidase digest. Four isomers of the Asp-X-type peptides (L- α -Asp-X, D- α -Asp-X, L- β -Asp-X, and D- β -Asp-X) were synthesized. The AccQ derivatives of synthetic peptides (std.) and peptides in RPH and its exopeptidase digest were analyzed using LC-MS/MS. Resolution of isomers of Asp-Phe, Asp-Ile/Leu, Asp-Glu, and Asp-Val by LC-MS/MS are shown in Figure 4a–d, respectively. L α , L β , D α , and D β represent peptides containing L- α -aspartyl residue, L- β -aspartyl residue, D- α -aspartyl residue, and D- β -aspartyl residue, respectively. Resolution between L- α -Asp-Ile and L- α -Asp-Leu, and between D- α -Asp-Ile and D- α -Asp-Leu, could not be performed under present condition.

dase digest was very low. PyroGlu-Lys, which contains an amino group in the side chain of the lysyl residue, may be transported via a basolateral transporter for other amino group-containing dipeptides. PyroGlu-Gln and pyroGlu-Glu in enterocytes may be transported back to the lumen. P-glycoprotein, which exist in the luminal membrane of Caco-2 cells, has been demonstrated to transport some drugs or peptides from the basolateral side to the apical side (Sharom, 2011), which may be involved in the back-transportation of pyroGlu-Gln and pyroGlu-Glu. These pyroglutamyl peptides may reach in the colon and undergo metabolization by microbes.

It has also been demonstrated that Pro-Hyp enhances the growth of fibroblasts from mouse skin (Shigemura et al., 2009; Asai et al., 2020) and Pro-Gly enhances the synthesis of elastin in normal human dermal fibroblasts (Shigemura et al., 2012). Collagen and elastin hydrolysate supplementation has been demonstrated to exert beneficial effects on humans, such as enhanced pressure ulcer healing and improved skin elasticity, respectively (Sugihara et al., 2018; Shiratsuchi et al., 2016). Taken together, food-derived Pro-Hyp and Pro-Gly in the blood can be responsible for the beneficial effects of oral administration of collagen and elastin hydrolysates. By contrast, the blood concentration of pyroGlu-Leu in the present study (≈ 70 nM) was considerably lower than that of

Pro-Hyp (Taga et al., 2019; Asai et al., 2019) and Pro-Gly (Shigemura et al., 2012). However, oral administration of pyroGlu-Leu has been demonstrated to exert significant beneficial effects, such as hepatoprotective effect at a dose of 20 mg/kg BW (Sato et al., 2013), attenuation of dextran sulfate sodium (DSS)-induced colitis and dysbiosis at dose of 0.1–1.0 mg/kg BW (Wada et al., 2013), and attenuation of high-fat diet-induced dysbiosis at a dose of 1.0 mg/kg BW (Shirako et al., 2019). Furthermore, it has been demonstrated that a mixture of pyroGlu-Leu, pyroGlu-Ile, and pyroGlu-Val, hydrophobic pyroglutamyl peptides in a one serve of fermented soy paste (miso) soup, attenuated high-fat diet-induced obesity (Shirako et al., 2020). No significant increase in blood pyroGlu-Leu levels was observed after oral administration of a such small dose (0.1 mg/kg BW). Thus, it is unlikely that such low concentrations of pyroGlu-Leu in the blood act directly on the target in the body. On the other hand, Shirako et al. demonstrated that pyroGlu-Leu enhanced the secretion of host antimicrobial peptides from Paneth cells in the ileum, which indicates that some pyroglutamyl peptides can exert biological activities by acting on cells in the gastrointestinal tract. The present study demonstrated a relatively high pyroGlu-Leu concentration in the lumen and ileal tissue after administration of RPH at a realistic dose, which suggests that RPH

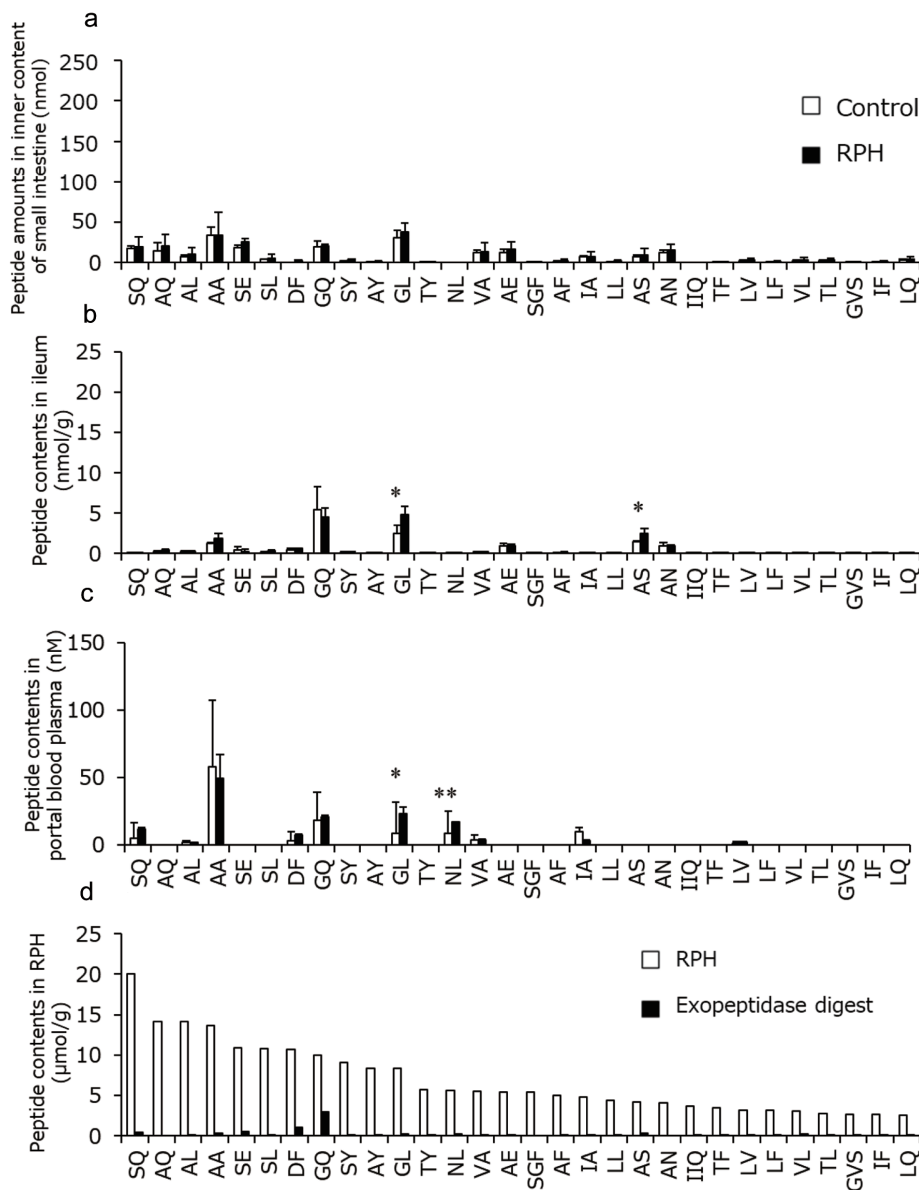


Figure 5. Amounts and concentrations of RPH-derived peptides containing amino group in rat (a) lumen, (b) ileal tissue, and (c) portal blood plasma before and after administration of RPH. These data are presented with peptide concentrations in RPH and its exopeptidase digest (d). Data are shown as mean ± standard deviation. (a–c, n = 3). Asterisks indicate that significant differences between values before and after administration of RPH as determined by *t*-test (**p* < 0.05, ***p* < 0.01).

supplementation might exert some beneficial effects attributable to pyroGlu-Leu. Further studies on the effects of RPH on high-fat diet-induced dysbiosis and obesity are currently underway.

5. Conclusion

Oral administration of RPH had little impact on the concentrations of the *in vitro* exopeptidase-susceptible peptides in the body, including the digestive tract. By contrast, most of the pyroglutamyl peptides in RPH that resisted *in vitro* exopeptidase digestion, significantly increased in concentration in the lumen and ileal tissue after oral administration of RPH. These results indicate that

in vitro exopeptidase digestion is useful for predicting which peptides can reach the target organs, allowing the bioactive peptides to be narrowed down. However, the concentrations of exopeptidase-resistant pyroglutamyl peptides increased slightly or did not increase in the blood of rats after oral administration. These findings suggest that the exopeptidase-resistant pyroglutamyl peptides can enter intestinal cells but are poorly transported into the blood flow. Thus, these pyroglutamyl peptides can act on cells in the gastrointestinal tracts, such as enterocytes, Paneth cells, goblet cells, and innate and acquired immune cells. Parts of the pyroglutamyl peptides may be transferred to the cecum and colon, where they are metabolized by microbes. The resultant metabolites may exert some bioactivity.

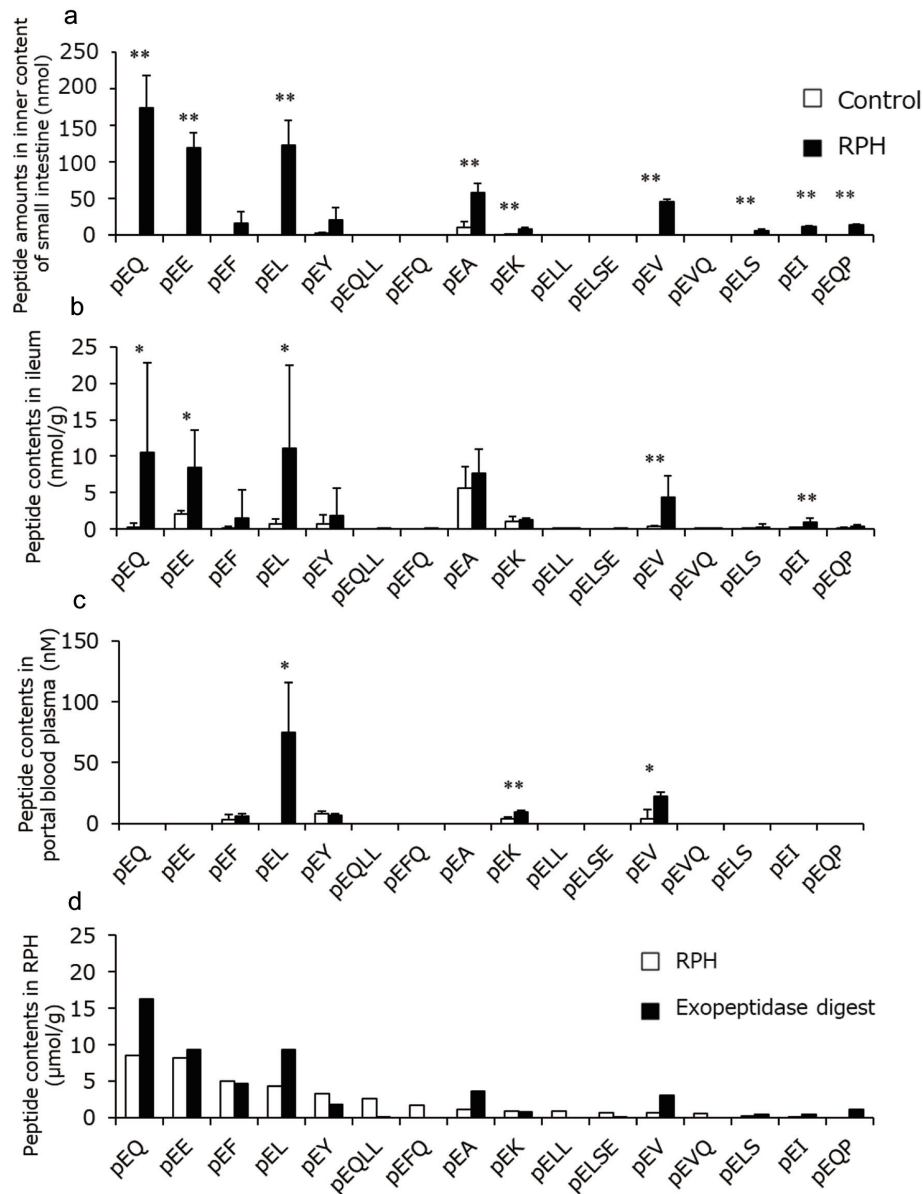


Figure 6. Amounts and concentrations of RPH-derived pyroglutamyl peptides in rat (a) lumen, (b) ileal tissue, and (c) portal blood plasma before and after administration of RPH. These data are presented with pyroglutamyl peptide concentrations in RPH and its exopeptidase digest (d). Data are shown as mean \pm standard deviation. (a–c, $n = 3$). Asterisks indicate that significant differences between values before and after administration of RPH as determined by *t*-test ($*p < 0.05$, $**p < 0.01$).

Acknowledgments

We would like to thank the Kyoto Louis Pasteur Center for Medical Research for allowing us to perform animal experiments. This work was supported by Commissioned Research between Kyoto University and Bansyu chomiryo Co., Ltd. (Project number 100191000003).

Conflict of interest

There are no conflicts of interest to declare.

Supplementary Material

Suppl 1. Elution patterns of peptides in (a) RPH and (b) its exopeptidase digest by size exclusion chromatography (SEC).

Suppl 2. Mass chromatograms of AccQ-derivatives of SEC fractions of RPH by precursor ion scan mode. Peaks marked with uppercase represent amino acids. Peaks marked with number represent AccQ-peptides. Number on peak corresponds with Table 1.

Suppl 3. Mass chromatograms of AccQ-derivatives of SEC frac-

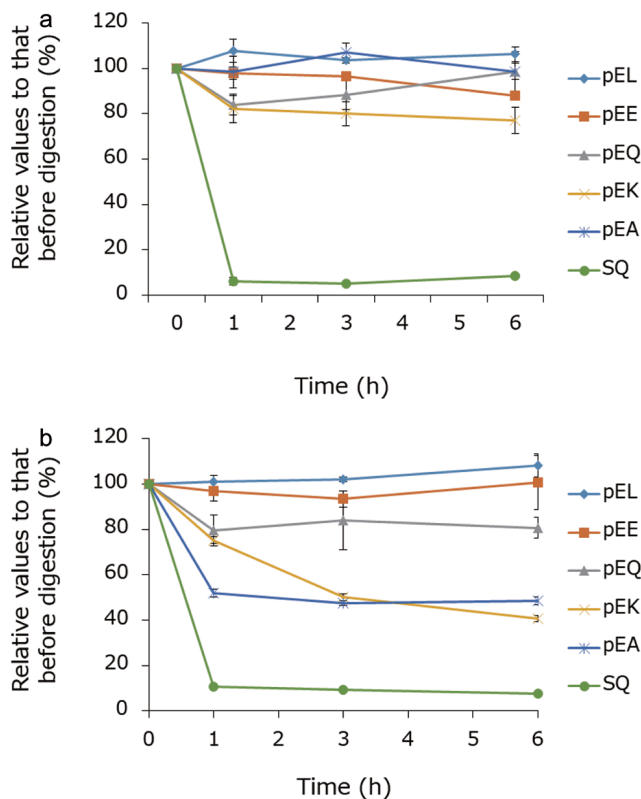


Figure 7. Susceptibility of some RPH-derived peptides to proteases in rat (a) ileal extract and (b) blood plasma.

tions of the exopeptidase digest of RPH by precursor ion scan mode. Peaks marked with uppercase represent amino acids. Peaks marked with number represent AccQ-peptides and AccQ-amino acid derivatives. Number on peak corresponds with Table 2.

Suppl 4. Mass chromatograms of pyroglutamyl peptides in SEC fractions of RPH by precursor ion scan mode. Peaks marked with number represent pyroglutamyl peptides. Number on peak corresponds with Table 3.

Suppl 5. Mass chromatograms of pyroglutamyl peptides in SEC fractions of the exopeptidase digest of RPH by precursor ion scan mode. Peaks marked with number represent pyroglutamyl peptides. Number on peak corresponds with Table 4.

Suppl 6. Mass chromatograms of non-derivatized peptides and amino acids in RPH (black line) and its exopeptidase digest (pink line) in total ion scan mode. Total ion scan was carried out at short scanning ranges of $m/z = 50\text{--}150$, $150\text{--}200$, $200\text{--}250$, $250\text{--}300$, $300\text{--}350$, $350\text{--}400$, $400\text{--}450$, $450\text{--}500$, $500\text{--}600$, $600\text{--}700$, $700\text{--}800$, and $800\text{--}1,000$, respectively.

References

- Aito-Inoue, M., Lackeyram, D., Fan, M.Z., Sato, K., and Mine, Y. (2007). Transport of a tripeptide, Gly-Pro-Hyp, across the porcine intestinal brush-border membrane. *J. Pept. Sci.* 13(7): 468–474.
- Aito-Inoue, M., Ohtsuki, K., Nakamura, Y., Eun, Y.P., Iwai, K., Morimatsu, F., and Sato, K. (2006). Improvement in isolation and identification of food-derived peptides in human plasma based on precolumn derivatization of peptides with phenyl isothiocyanate. *J. Agric. Food Chem.* 54(15): 5261–5266.
- Aluko, R.E. (2015). Antihypertensive peptides from food proteins. *Annu. Rev. Food Sci. Technol.* 6: 235–262.
- Asai, T., Takahashi, A., Ito, K., Uetake, T., Matsumura, Y., Ikeda, K., Inagaki, N., Nakata, M., Imanishi, Y., and Sato, K. (2019). Amount of collagen in the meat contained in Japanese daily dishes and the collagen peptide content in human blood after ingestion of cooked fish meat. *J. Agric. Food Chem.* 67(10): 2831–2838.
- Asai, T.T., Yoshikawa, K., Sawada, K., Fukamizu, K., Koyama, Y.-I., Shigemura, Y., Jimi, S., and Sato, K. (2020). Mouse skin fibroblasts with mesenchymal stem cell marker p75 neurotrophin receptor proliferate in response to prolyl-hydroxyproline. *J. Funct. Foods.* 66(1): 103792.
- Bidlingmeyer, B.A., Cohen, S.A., and Tarvin, T.L. (1984). Rapid analysis of amino acids using pre-column derivatization. *J. Chromatogr.* 336(1): 93–104.
- Chakrabarti, S., Guha, S., and Majumder, K. (2018). Food-derived bioactive peptides in human health: Challenges and opportunities. *Nutrients.* 10(11): 1738.
- Chen, L., Ejima, A., Gu, R., Lu, J., Cai, M., and Sato, K. (2019). Presence of exopeptidase-resistant and susceptible peptides in a bacterial protease digest of corn gluten. *J. Agric. Food Chem.* 67(43): 11948–11954.
- Dong, J.Y., Szeto, I.M.Y., Makinen, K., Gao, Q., Wang, J., Qin, L.Q., and Zhao, Y. (2013). Effect of probiotic fermented milk on blood pressure: A meta-analysis of randomized controlled trials. *Br. J. Nutr.* 110(7): 1188–1194.
- Ejima, A., Nakamura, M., Suzuki, Y.A., and Sato, K. (2018). Identification of food-derived peptides in human blood after ingestion of corn and wheat gluten hydrolysates. *J. Food Bioact.* 2: 104–111.
- Ejima, A., Yamada, K., and Sato, K. (2019). Presence of aspartic dipeptides with β peptide bond and/or D-aspartyl residue in rat blood after ingestion of porcine liver protein hydrolysate. *Bioact. Compd. Heal. Dis.* 2(7): 155–169.
- Iwai, K., Hasegawa, T., Taguchi, Y., Morimatsu, F., Sato, K., Nakamura, Y., Higashi, A., Kido, Y., Nakabo, Y., and Ohtsuki, K. (2005). Identification of food-derived collagen peptides in human blood after oral ingestion of gelatin hydrolysates. *J. Agric. Food Chem.* 53(16): 6531–6536.
- Kawasaki, T., Seki, E., Osajima, K., Yoshida, M., Asada, K., Matsui, T., and Osajima, Y. (2000). Antihypertensive effect of Valyl-Tyrosine, a short chain peptide derived from sardine muscle hydrolyzate, on mild hypertensive subjects. *J. Hum. Hypertens.* 14(8): 519–523.
- Lee, S.Y., and Hur, S.J. (2017). Antihypertensive peptides from animal products, marine organisms, and plants. *Food Chem.* 228: 506–517.
- Liao, W., Bhullar, K.S., Chakrabarti, S., Davidge, S.T., and Wu, J. (2018). Egg white-derived tripeptide IRW (Ile-Arg-Trp) is an activator of angiotensin converting enzyme 2. *J. Agric. Food Chem.* 66(43): 11330–11336.
- Matsui, T., Imamura, M., Oka, H., Osajima, K., Kimoto, K.I., Kawasaki, T., and Matsumoto, K. (2004). Tissue distribution of antihypertensive dipeptide, Val-Tyr, after its single oral administration to spontaneously hypertensive rats. *J. Pept. Sci.* 10(9): 535–545.
- Papayannopoulos, I.A. (1995). The interpretation of collision-induced dissociation tandem mass spectra of peptides. *Mass Spectrom Rev.* 14(1): 49–73.
- Sanderink, G.J., Artur, Y., and Siest, G. (1988). Human aminopeptidases: A review of the literature. *Clin. Chem. Lab. Med.* 26(12): 795–808.
- Sato, K. (2022). Metabolic Fate and Bioavailability of Food-Derived Peptides: Are Normal Peptides Passed through the Intestinal Layer to Exert Biological Effects via Proposed Mechanisms? *J. Agric. Food Chem.* 70(5): 1461–1466.
- Sato, K., Egashira, Y., Ono, S., Mochizuki, S., Shimmura, Y., Suzuki, Y., Nagata, M., Hashimoto, K., Kiyono, T., Park, E.Y., Nakamura, Y., Itabashi, M., Sakata, Y., Furuta, S., and Sanada, H. (2013). Identification of a hepatoprotective peptide in wheat gluten hydrolysate against d-galactosamine-induced acute hepatitis in rats. *J. Agric. Food Chem.* 61(26): 6304–6310.
- Sato, K., Nisimura, R., Suzuki, Y., Motoi, H., Nakamura, Y., Ohtsuki, K., and Kawabata, M. (1998). Occurrence of indigestible pyroglutamyl peptides in an enzymatic hydrolysate of wheat gluten prepared on an industrial scale. *J. Agric. Food Chem.* 46(9): 19–21.
- Sharom, F.J. (2011). The P-glycoprotein multidrug transporter. *Essays Biochem.* 50(1): 161–178.

- Shen, W., and Matsui, T. (2017). Current knowledge of intestinal absorption of bioactive peptides. *Food Funct.* 8(12): 4306–4314.
- Shigemura, Y., Iwai, K., Morimatsu, F., Iwamoto, T., Mori, T., Oda, C., Taira, T., Park, E.Y., Nakamura, Y., and Sato, K. (2009). Effect of prolyl-hydroxyproline (Pro-Hyp), a food-derived collagen peptide in human blood, on growth of fibroblasts from mouse skin. *J. Agric. Food Chem.* 57(2): 444–449.
- Shigemura, Y., Nakaba, M., Shiratsuchi, E., Suyama, M., Yamada, M., Kiyono, T., Fukamizu, K., Park, E.Y., Nakamura, Y., and Sato, K. (2012). Identification of food-derived elastin peptide, prolyl-glycine (Pro-Gly), in human blood after ingestion of elastin hydrolysate. *J. Agric. Food Chem.* 60(20): 5128–5133.
- Shirako, S., Kojima, Y., Hasegawa, T., Yoshikawa, T., Matsumura, Y., Ikeda, K., Inagaki, N., and Sato, K. (2020). Identification of short-chain pyroglutamyl peptides in Japanese salted fermented soy paste (miso) and their anti-obesity effect. *J. Food Bioact.* 12: 129–139.
- Shirako, S., Kojima, Y., Tomari, N., Nakamura, Y., Matsumura, Y., Ikeda, K., Inagaki, N., and Sato, K. (2019). Pyroglutamyl leucine, a peptide in fermented foods, attenuates dysbiosis by increasing host antimicrobial peptide. *NPJ Sci. Food.* 3(18): 203778568.
- Shiratsuchi, E., Nakaba, M., and Yamada, M. (2016). Elastin hydrolysate derived from fish enhances proliferation of human skin fibroblasts and elastin synthesis in human skin fibroblasts and improves the skin conditions. *J. Sci. Food Agric.* 96(5): 1672–1677.
- Skopicki, H.A., Fisher, K., Zikos, D., Flouret, G., Bloch, R., Kubillus, S., and Peterson, D.R. (1998). Carrier-mediated transport of pyroglutamyl-histidine in renal brush border membrane vesicles. *Am. J. Physiol.* 255(6 Pt 1): C822–C827.
- Sugihara, F., Inoue, N., and Venkateswarathirukumara, S. (2018). Ingestion of bioactive collagen hydrolysates enhanced pressure ulcer healing in a randomized double-blind placebo-controlled clinical study. *Sci. Rep.* 8(1): 11403.
- Taga, Y., Iwasaki, Y., Shigemura, Y., and Mizuno, K. (2019). Improved in vivo tracking of orally administered collagen hydrolysate using stable isotope labeling and LC-MS techniques. *J. Agric. Food Chem.* 67(16): 4671–4678.
- Tanaka, M., Matsui, T., Ushida, Y., and Matsumoto, K. (2006). Vasodilating effect of di-peptides in thoracic aortas from spontaneously hypertensive rats. *Biosci. Biotechnol. Biochem.* 70(9): 2292–2295.
- Wada, S., Sato, K., Ohta, R., Wada, E., Bou, Y., Fujiwara, M., Kiyono, T., Park, E.Y., Aoi, W., Takagi, T., Naito, Y., and Yoshikawa, T. (2013). Ingestion of low dose pyroglutamyl leucine improves dextran sulfate sodium-induced colitis and intestinal microbiota in mice. *J. Agric. Food Chem.* 61(37): 8807–8813.
- Yang, Y., Marczak, E.D., Yokoo, M., Usui, H., and Yoshikawa, M. (2003). Isolation and antihypertensive effect of angiotensin I-converting enzyme (ACE) inhibitory peptides from spinach Rubisco. *J. Agric. Food Chem.* 51(17): 4897–4902.
- Yoshikawa, M., Fujita, H., Matoba, N., Takenaka, Y., Yamamoto, T., Yamauchi, R., Tsuruki, H., and Takahata, K. (2000). Bioactive peptides derived from food proteins preventing lifestyle-related diseases. *BioFactors.* 12: 143–146.